SAR Image Compression using Optimum Threshold based Support Vector Machines

Kaushik K[†] and Manikandan J[‡]
[†]Department of Telecommunication Engineering, [‡]Department of ECE and Crucible of Research and Innovation (CORI),
PES University, 100-Feet Ring Road, BSK Stage III, Bangalore 560085, Karnataka, INDIA.
{email : kaushik.koneripalli@gmail.com, manikandanj@pes.edu}

***Abstract*— Synthetic Aperture Radar (SAR) systems used on an unmanned aerial vehicle (UAV), aircraft or spacecraft are used to build SAR images using the concepts of backscattering. SAR images consist of high-resolution reflected returns of radar frequency energy from terrain illuminated by directed beam of pulses generated by the SAR system. In the case of aircrafts, these SAR images are displayed on the cockpit, transmitted to ground station as well as stored in on-board storage disks. SAR images serve as vital source of information for a large variety of applications which includes reconnaissance, automatic target recognition and mapping of geographical area. There is an urge to compress SAR images which would in turn reduce the transmission time of SAR images from on-board systems to ground station. SAR image compression will also reduce the memory requirements on-board. In this paper, two approaches for SAR image compression using optimum threshold based Support Vector Machine (SVM) regression are proposed. The first approach uses only proposed SVM regression, whereas the second approach is a two-stage SAR image compression using standard 1-level wavelet decomposition followed by proposed SVM regression. In order to assess the efficacy of the proposed system, datasets from USC-SIPI image databases are employed and 67.81 – 77.36% image compression is achieved with a PSNR ranging between 36.20dB and 43.12dB.**

Keywords- Image Compression; SAR; Support Vectors; Support Vector Machines; Wavelets.

I. INTRODUCTION

Machine learning applications are expected to provide new breakthroughs that will amplify human abilities in taking correct and timely decisions to solve several seemingly unsolvable problems with innovative algorithms and techniques. Several machine learning algorithms have evolved over years with Support Vector Machines (SVM) and Relevance Vector Machines (RVM) considered as the most commonly used ones in recent years. SVM employs statistical inference, whereas RVM employs Bayesian inference. SVM is used for spam categorization in [1], speech recognition in [2], for Internet of Things (IoT) environment in [3], biometric systems in [4] and many more. Similarly RVM is also used for various applications such as gear fault detection in [5], face detection in [6], non-linear dynamic compensation of sensors in [7], personal authentication system in [8] and many more.

The motivation towards reducing the on-board memory storage requirements and data transmission to ground station has led to the development of algorithms for SAR image compression pertaining to aerospace and satellite applications. SAR image compression using K-nearest neighbour based Lee filter and wavelet is reported in [9], using multiscale dictionary learning and sparse representation in [10], using steganography in [11], using human visual system model in [12] and using RVM in [13].

The block diagram of proposed system is shown in Fig. 1. SAR images are built on-board using the backscatters received from ground/terrain. The SAR images built are displayed on the cockpit (in the case of manned aircrafts only), used by on-board automatic target recognition system, on-board storage for future analysis and transmission to ground station. The SAR images are compressed before storing it onto the on-board memory and transmitting. In this paper, SAR image compression using optimum threshold based SVM with and without wavelets is proposed and their performance is evaluated.

The organization of the paper is as follows: Section II provides an overview of wavelet decomposition and Section III explains the SVM regression and the proposed optimum threshold based SVM technique. Experimental results of proposed system are reported in Section IV, followed by conclusion and references.

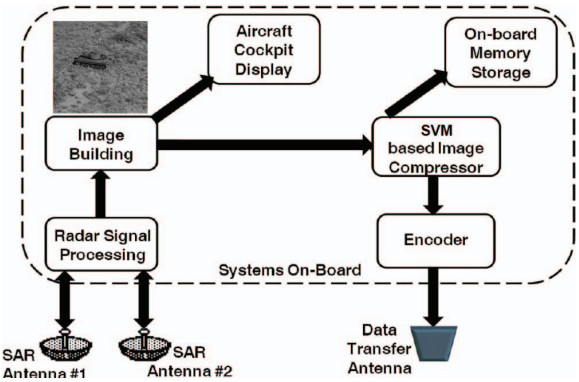

Fig. 1. Block diagram of proposed SAR Image Compression System

II. WAVELET DECOMPOSITION

A wavelet is a mathematical function used for digital signal processing and image compression. 1-D wavelet decomposition is used for one-dimensional signals such as

978-1-5090-3646-2/16/$31.00 ©2016 IEEE

speech and 2-D wavelet decomposition is used for image processing and compression. Discrete wavelet transform (DWT) on an image is performed using 1-D DWT row-wise, followed by 1-D DWT column-wise as shown in Fig. 2. The first level, second level and third level wavelet decompositions of a SAR image is shown in Fig. 3.

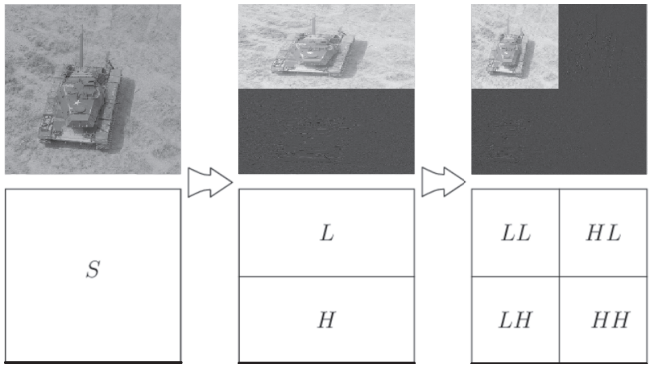

Fig. 2. Illustration of 2D DWT on a SAR image

Fig. 3. First, Second and Third Level Wavelet Decomposition of SAR image

The 2-D DWT of an image f(x,y) comprises of four components (Approximation, Horizontal, Vertical and Diagonal) and is given as

$$f(x,y) = \frac{1}{\sqrt{MN}} \sum_m \sum_n W_\phi(j_o,m,n)\phi_{j_o,m,n}(x,y) + \frac{1}{\sqrt{MN}} \sum_{i=H,V,D} \sum_{j=j_o}^{\infty} \sum_m \sum_n W_\psi^i(j_o,m,n)\, \Psi^i_{j,m,n}(x,y) \quad (1)$$

where j_o is the level of decomposition, M denotes the number of points along the x direction, N denotes the number of points along the y direction. $\Psi^i_{j,m,n}(x,y)$ and $\phi_{j,m,n}(x,y)$ are the wavelet and scaling orthonormal basis functions respectively obtained by the shifted and scaled versions of the wavelet and scaling functions given as

$$\psi^i_{j,m,n}(x,y) = 2^{j/2}\, \psi^i(2^j x - m, 2^j y - n) \qquad i = \{H,V,D\} \quad (2)$$

$$\phi_{j,m,n}(x,y) = 2^{j/2}\, \phi(2^j x - m, 2^j y - n) \quad (3)$$

$W_\phi(j_o,m,n)$ and $W_\psi^i(j_o,m,n)$ denote the approximation and detailed components given as

$$W_\phi(j_o,m,n) = \frac{1}{\sqrt{MN}} \sum_{x=0}^{M-1} \sum_{y=0}^{N-1} f(x,y)\, \phi_{j_o,m,n}(x,y) \quad (4)$$

$$W_\psi^i(j_o,m,n) = \frac{1}{\sqrt{MN}} \sum_{x=0}^{M-1} \sum_{y=0}^{N-1} f(x,y)\, \Psi^i_{j,m,n}\,, \; i = \{H,V,D\} \quad (5)$$

The decomposition of SAR image using DWT and represented using filter banks is shown in Fig. 4. More details about wavelet transform can be had from [14, 15].

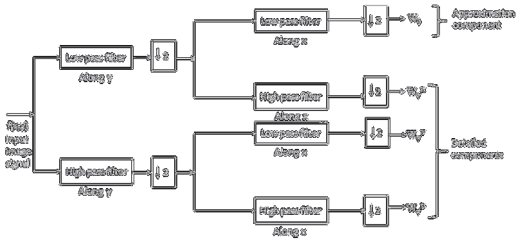

Fig. 4. Illustration of 2D DWT using Filter Banks

III. SUPPORT VECTOR MACHINES

Support Vector Machine (SVM) is used for regression and classification problems. A brief overview of SVM regression employed for proposed work is reported in this section. The basic idea of SVM regression is to predict the given function within a predefined error threshold ϵ. A two dimensional image can be converted into a one dimensional dataset as $\{\boldsymbol{x_i}, \boldsymbol{y_i}\}_{i=1}^{N}$, where $\boldsymbol{y_i}$ is the target output for training data $\boldsymbol{x_i}$, and N denotes the number of datapoints.

The line of approximation using training datasets is given as $\boldsymbol{y}' = \mathbf{w}\varphi(x) + b$ where $\mathbf{w}$ is the weight matrix, $\varphi(x)$ is the mapping function and b is the bias. An error margin ϵ is defined such that for any predicted data $\boldsymbol{y_i}'$, $(\boldsymbol{y_i} - \boldsymbol{y_i}') \leq \pm\, \epsilon$. The error function is given as

$$\tfrac{1}{2}\|w\|^2 + C\sum_{i=1}^{N} \left(\xi_i^+ + \xi_i^-\right) \quad (6)$$

where C is the penalty parameter, ξ_i^+ is the slack variable penalty when the training sample lies outside and above the epsilon insensitive tube and ξ_i^- is the slack variable penalty when the training sample lies outside and below the epsilon insensitive tube. On minimizing the error function, a set of Lagrange multipliers α^+ and α^- is obtained for each training data with equations for $\mathbf{w}$ and b given as

$$w = \sum_{i=1}^{N} (\alpha_i^+ - \alpha_i^-)\varphi(x_i) \quad (7)$$

$$b = \frac{1}{N} \sum_{i=1}^{N} (yi - \varepsilon - \sum_{m=1}^{N} (\alpha_i^+ - \alpha_i^-)\, K(x_i, x_m)) \quad (8)$$

The SVM regression/prediction equation is given as

$$y' = \sum_{m=1}^{N} (\alpha_i^+ - \alpha_i^-)\, K(x_i, x') + b \quad (9)$$

where x'is the input test data, $K(x_i,x') = \langle \varphi(x_i) \cdot \varphi(x') \rangle$ is the Kernel function and y' is the predicted output.

The value $(\alpha_i^+ - \alpha_i^-)$ is non-zero for all support vectors and all the support vectors are employed to build the regression model. An attempt is made to prune the number of support vectors required by the SVM model, using an optimum threshold technique that employs the support vectors satisfying the condition $(\alpha_i^+ - \alpha_i^-) \leq \alpha_{threshold}$. Optimum threshold is the $\alpha_{threshold}$ value for which nil or negligible degradation is observed.

IV. EXPERIMENTAL RESULTS

The performance of proposed image compression system using optimum threshold based SVM model is reported in this section. In order to assess the performance of proposed work, six images from USC-SIPI Image database [16] are used, which are shown in Fig. 5. These images are fed to proposed SVM based image compression block with Gaussian kernel as the mapping function. Two variants of SVM based image compression block are evaluated in the proposed work. The first approach converts the 2D image into 1D signal and proposed SVM regression is used row-wise for sparse representation of the 1D signal. The second approach uses a combination of wavelet and proposed SVM regression, wherein one-level wavelet decomposition is performed on the SAR images and the wavelet coefficients are approximated using optimum threshold based SVM regression. Finally, the image is reconstructed on the receiver end based on the compression approach used. The metric considered in this paper to measure the quality of reconstructed images is the Peak Signal to Noise Ratio (PSNR), which is given as

$$PSNR = 10 \cdot log_{10}(\frac{255^2}{MSE}) \quad (10)$$

where MSE is the mean square error (MSE) given as

$$MSE = \frac{1}{N \cdot N} \sum_{i=0}^{N-1} \sum_{j=0}^{N-1} [I(i,j) - I'(i,j)]^2 \quad (11)$$

where $I(i,j)$ is the original image and $I'(i,j)$ is the reconstructed image.

The effectiveness of proposed image compression system using the images given in Fig. 5 is evaluated by compressing the SAR images using only a subset of SVs corresponding to those hyperparameters whose value is lesser than a threshold (i.e., $(\alpha_i^+ - \alpha_i^-) \leq \alpha_{\text{threshold}}$). It may be noted that $(\alpha_i^+ - \alpha_i^-) \in [-C, C]$. The evaluation results for SVM based image compression with C =1 are reported in Table I with all the images reduced to a size of 256x256 pixels. It may be observed from Table I that as the $\alpha_{\text{threshold}}$ value decreases, the number of support vectors (SVs) also decreases, whereas a maximum PSNR value is obtained for $\alpha_{\text{threshold}} = 0$ for all the images considered in this paper for experimentation. The evaluation results for wavelet and SVM based image compression with C =1 are reported in Table II using 512x512 sized images and one-level wavelet decomposition. It is observed from Table II that as the $\alpha_{\text{threshold}}$ value decreases, the number of support vectors (SVs) also decreases, whereas a maximum PSNR value is obtained with $\alpha_{\text{threshold}} = 0$ for this case too. The experimental results confirm that the proposed optimum threshold SVM based image compression holds good for all the images considered for evaluation.

The reconstructed images with $\alpha_{\text{threshold}} = -0.4$ are shown in Fig. 6. The images reconstructed with negligible degradation are shown in first column and the second column shows image reconstructed with minor visible degradations. For automatic target recognition, these reconstructed images provide sufficient information to detect target using edge detection techniques as reported in [17].

Details about the amount of compression achieved on using the proposed optimum threshold SVM based SAR image compression system is reported in Table III. It may be observed from Table III that significant image compression is achieved on using proposed optimum threshold based SVM classifier.

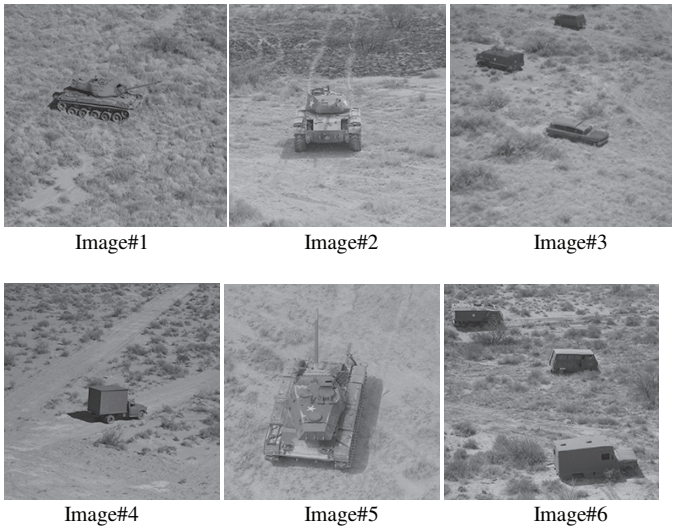

Fig. 5. Images used for the proposed work

TABLE I. PERFORMANCE EVALUATION OF PROPOSED IMAGE COMPRESSION SYSTEM USING SVM

$\alpha_{\text{threshold}}$	Image #1		Image #2		Image #3		Image #4		Image #5		Image #6	
	# SVs	PSNR	# SVs	PSNR	# SVs	PSNR	# SVs	PSNR	# SVs	PSNR	# SVs	PSNR
1.0	65536	32.93	65536	32.86	65536	32.55	65536	32.57	65536	32.29	65536	30.90
0.5	49626	35.31	49142	35.22	50841	35.06	51734	34.72	49708	36.55	51521	33.91
0.4	46079	36.07	45596	36.22	46325	35.97	46056	36.01	44497	38.15	46518	34.47
0.3	42495	36.94	41781	37.33	41548	37.34	40237	38.05	39797	40.08	41341	35.12
0.2	38877	37.71	37907	38.15	37073	38.60	35011	39.62	35507	41.69	36514	35.68
0.1	35293	38.26	34093	38.62	32835	39.36	30770	40.35	31591	42.55	31995	36.06
0.0	**31666**	**38.45**	**30252**	**38.78**	**29155**	**39.59**	**27245**	**40.60**	**27994**	**42.85**	**28027**	**36.20**
-0.1	28224	38.28	26804	38.68	25745	39.41	24099	40.39	24861	42.65	24353	36.05
-0.2	24783	37.78	23497	38.28	22609	38.87	21363	39.83	21806	41.90	21123	35.68
-0.3	21625	37.03	20428	37.71	19763	38.03	18717	39.06	18989	40.75	18268	35.09
-0.4	18748	36.22	17593	36.96	17111	37.06	16514	38.14	16502	39.27	15660	34.41
-0.5	16198	35.28	15055	36.10	14635	36.12	14273	36.99	14393	37.91	13518	33.68
-1.0	0	28.99	0	29.02	30	28.51	0	28.78	0	29.00	0	28.29

TABLE II. PERFORMANCE EVALUATION OF PROPOSED IMAGE COMPRESSION SYSTEM USING WAVELET AND SVM

$\alpha_{threshold}$	Image #1		Image #2		Image #3		Image #4		Image #5		Image #6	
	# SVs	PSNR	# SVs	PSNR	# SVs	PSNR	# SVs	PSNR	# SVs	PSNR	# SVs	PSNR
1.0	69169	31.93	69169	31.9	69169	32.5	69169	32.15	69169	31.79	69169	30.56
0.9	59263	34.14	61378	33.44	63108	34.14	63641	33.2	61551	33.92	60423	33.44
0.7	54332	35.48	56539	34.83	57995	35.67	59083	34.51	56467	36.33	55685	34.31
0.5	48424	37.07	50134	36.77	50883	37.46	51305	36.79	49512	38.63	49871	35.14
0.3	42119	38.84	42678	38.46	42686	39.71	41583	39.75	41912	41.14	43605	36.29
0.1	35715	39.98	35249	39.49	34770	41.33	32982	41.62	34757	42.69	37041	37.15
0.0	**32474**	**40.32**	**31796**	**39.77**	**31071**	**41.69**	**29548**	**42.02**	**31404**	**43.12**	**33875**	**37.33**
-0.1	29487	39.98	28590	39.49	27691	41.36	26602	41.67	28628	42.68	30871	37.14
-0.2	26606	39.57	25645	39.15	24442	40.80	23910	41.27	25197	42.13	27908	36.79
-0.3	23891	38.92	22893	38.62	21527	39.94	21359	40.55	22413	41.29	25052	36.27
-0.4	21322	38.08	20302	37.92	18966	38.93	19006	39.62	19843	40.22	22264	35.55
-0.5	18965	37.16	17906	37.09	16765	37.94	16786	38.49	17432	38.84	19440	34.66
-1.0	0	28.75	0	28.78	0	28.39	0	28.53	0	28.87	0	28.22

$\alpha_{threshold} = -0.3$ $\alpha_{threshold} = -0.4$

(a) Image #1

$\alpha_{threshold} = -0.3$ $\alpha_{threshold} = -0.4$

(b) Image #2

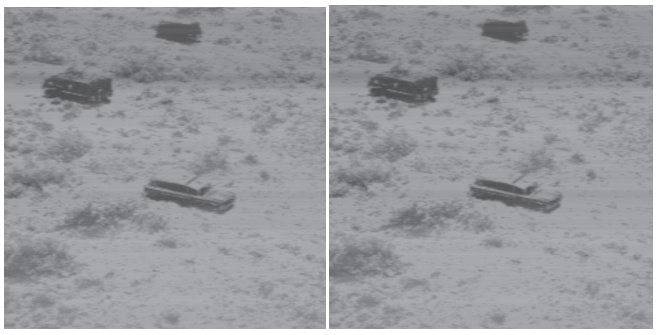

$\alpha_{threshold} = -0.3$ $\alpha_{threshold} = -0.4$

(c) Image #3

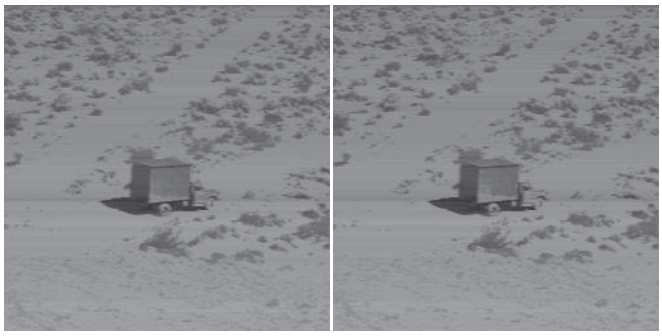

$\alpha_{threshold} = -0.3$ $\alpha_{threshold} = -0.4$

(d) Image #4

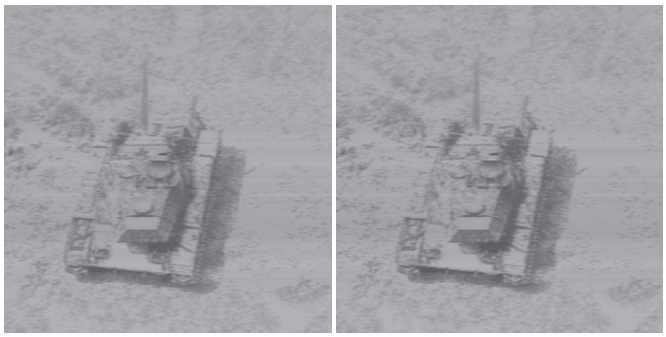

$\alpha_{threshold} = -0.3$ $\alpha_{threshold} = -0.4$

(e) Image #5

$\alpha_{threshold} = -0.3$ $\alpha_{threshold} = -0.4$

(f) Image #6

Fig. 6. Reconstructed Images for different $\alpha_{threshold}$ values

TABLE III. IMAGE COMPRESSION OBTAINED BY PROPOSED SYSTEM USING OPTIMUM THRESHOLD BASED SVM CLASSIFIER

$\alpha_{threshold}$	Image Compression Achieved (%)											
	Image #1		Image #2		Image #3		Image #4		Image #5		Image #6	
	SVM	DWT+SVM	SVM	DWT+SVM	SVM	DWT+SVM	SVM	DWT+SVM	SVM	DWT+SVM	SVM	DWT+SVM
1.0	0	0	0	0	0	0	0	0	0	0	0	0
0.9	12.20	14.32	12.48	11.26	10.70	8.760	8.51	7.990	8.74	11.01	8.57	12.64
0.7	18.78	21.45	19.58	18.26	16.18	16.15	13.48	14.58	14.91	18.36	14.40	19.49
0.5	28.25	29.99	28.95	27.52	26.50	26.44	25.21	25.83	28.14	28.42	25.51	27.90
0.3	38.56	39.11	39.60	38.30	39.93	38.29	41.83	39.88	42.46	39.41	40.23	36.96
0.1	48.98	48.37	50.71	49.04	52.53	49.73	55.51	52.32	54.33	49.75	53.74	46.45
0.0	54.22	53.05	56.26	54.03	57.85	55.08	60.61	57.28	59.53	54.60	59.48	51.03
-0.1	59.20	57.37	61.25	58.67	62.78	59.97	65.16	61.54	64.06	58.61	64.79	55.37
-0.2	64.17	61.53	66.03	62.92	67.31	64.66	69.11	65.43	68.47	63.57	69.46	59.65
-0.3	68.74	65.46	70.47	66.90	71.43	68.88	72.94	69.12	72.55	67.60	73.59	63.78
-0.4	**72.90**	**69.17**	**74.57**	**70.65**	**75.26**	**72.58**	**76.13**	**72.52**	**76.14**	**71.31**	**77.36**	**67.81**
-0.5	76.58	72.58	78.23	74.11	78.84	75.76	79.37	75.73	79.19	74.80	80.46	71.89
-0.9	91.45	83.75	89.00	85.43	89.84	85.97	89.57	86.01	89.11	85.59	89.31	87.23
-1.0	100.0	100.0	100.0	100.0	100.0	100.0	100.0	100.0	100.0	100.0	100.0	100.0

TABLE IV. PERFORMANCE EVALUATION OF PROPOSED SYSTEM USING OPTIMUM THRESHOLD BASED SVM CLASSIFIER FOR DIFFERENT WAVELETS

Wavelet	Image #1		Image #2		Image #3		Image #4		Image #5		Image #6	
	#SVs	PSNR	#SVs	PSNR	#SVs	PSNR	#SVs	PSNR	#SVs	PSNR	#SVs	PSNR
db1	18093	35.12	17410	35.54	15955	36.36	16671	37.20	16794	37.50	19102	33.67
db5	18738	35.49	18042	35.98	16569	36.67	17436	37.63	17495	37.99	19850	33.94
db10	19699	35.51	18881	36.04	17266	36.59	18134	37.47	18303	38.15	20475	33.93
db15	20432	35.46	19524	36.06	18062	36.56	18910	37.36	19058	38.20	21288	33.93
db20	21279	35.44	20480	36.14	18693	36.52	19712	37.30	19909	38.30	21966	33.91
db25	22048	35.37	21141	36.10	19461	36.46	20385	37.15	20694	38.38	22757	33.91
db30	22880	35.40	22022	36.13	20128	36.37	21342	37.14	21526	38.43	23503	33.87
db35	23700	35.40	22776	36.14	20896	36.28	21929	37.01	22330	38.47	24371	33.90
db40	24502	35.40	23687	36.14	21755	36.22	22746	36.97	23107	38.47	25200	33.90
db41	24684	35.40	23906	36.16	21925	36.20	22903	36.98	23398	38.50	25413	33.91
db42	24886	35.40	24086	36.17	22046	36.17	23004	36.96	23569	38.50	25515	33.92
db43	25037	35.39	24191	36.18	22241	36.16	23120	36.93	23761	38.51	25719	33.93
db44	25269	35.41	24370	36.19	22340	36.13	23305	36.90	23866	38.51	25910	33.94
db45	25372	35.40	24528	36.18	22499	36.11	23436	36.86	24019	38.47	26149	33.92
sym2	18327	35.43	17588	35.79	16083	36.59	16844	37.52	16873	37.82	19311	33.84
sym5	18776	35.48	18069	35.91	16622	36.64	17436	37.62	17387	38.00	19796	33.88
sym10	19679	35.50	18694	36.03	17274	36.64	18055	37.54	18191	38.14	20584	33.96
sym15	20410	35.49	19422	36.03	18070	36.59	19022	37.56	18825	38.20	21366	33.88
sym20	21188	35.46	20124	36.08	18693	36.49	19639	37.45	19510	38.31	21872	33.84
sym25	21962	35.39	20770	36.07	19442	36.44	20400	37.40	20198	38.33	22714	33.84
bior1.1	18093	35.12	17410	35.54	15955	36.36	16671	37.20	16794	37.50	19102	33.67
meyer	26441	35.32	24813	36.03	23079	36.20	24286	37.07	24150	38.51	27061	33.75
bior1.3	18547	35.44	17838	35.83	16381	36.64	17050	37.47	17055	37.81	19615	33.90
bior1.5	18963	35.54	18210	35.95	16749	36.74	17387	37.55	17407	37.96	20009	33.99
bior2.2	19324	36.45	18543	36.70	17057	37.61	17419	38.42	17895	38.79	20331	34.54
bior2.4	19772	36.61	18834	36.82	17402	37.70	17808	38.52	18269	38.99	20708	34.62
bior2.6	20175	36.70	19178	36.92	17758	37.76	18166	38.60	18615	39.10	21110	34.68
bior2.8	20550	36.75	19486	36.98	18088	37.79	18567	38.65	18978	39.19	21457	34.72
bior3.1	20418	38.21	19496	38.01	**18242**	**39.19**	18151	39.78	18971	40.18	**21440**	**35.67**
bior3.3	20599	38.12	19742	37.97	18398	39.07	18366	39.72	19222	40.21	21568	35.56
bior3.5	20943	38.17	19990	37.99	18659	39.03	18672	39.75	19496	40.28	21893	35.58
bior3.7	21322	38.22	20302	38.02	18966	39.04	19006	39.78	19843	40.40	22264	35.61
bior3.9	**21687**	**38.26**	**20632**	**38.08**	19336	39.06	**19352**	**39.79**	**20185**	**40.48**	22606	35.62
bior4.4	19050	35.48	18169	35.95	16635	36.66	17326	37.50	17538	37.94	19896	33.91
bior5.5	18432	34.69	17617	35.27	16270	35.92	17171	36.76	17109	37.25	19379	33.40
bior6.8	19719	35.69	18802	36.17	17274	36.81	17999	37.72	18131	38.23	20625	34.05

The performance of proposed SAR image compression system using optimum threshold based SVM and wavelets is assessed using different wavelets and their results are reported in Table IV with $\alpha_{threshold} = -0.4$. It is observed from Table IV that the proposed system performed satisfactorily for all types of wavelets with biorthogonal wavelets providing best PSNR for all the images. Details about the percentage of image compression achieved on using different wavelets are reported in Table V and a maximum of 76.12% image compression is obtained for various images considered in the work with biorthogonal 5.5 wavelet providing maximum compression for all the images considered.

TABLE V. IMAGE COMPRESSION OBTAINED BY PROPOSED SYSTEM FOR DIFFERENT WAVELETS

Wavelet	Image #1	Image #2	Image #3	Image #4	Image #5	Image #6
db1	72.39%	73.43%	75.65%	74.56%	74.37%	70.85%
db5	72.28%	73.31%	75.49%	74.21%	74.12%	70.64%
db10	71.95%	73.11%	75.41%	74.18%	73.94%	70.84%
db15	71.97%	73.22%	75.22%	74.06%	73.86%	70.80%
db20	71.86%	72.92%	75.28%	73.93%	73.67%	70.95%
db25	71.88%	73.03%	75.18%	74.00%	73.60%	70.97%
db30	71.83%	72.89%	75.22%	73.72%	73.50%	71.06%
db35	71.82%	72.92%	75.15%	73.93%	73.45%	71.02%
db40	71.84%	72.78%	75.00%	73.86%	73.45%	71.04%
db41	71.83%	72.72%	74.98%	73.86%	73.29%	71.00%
db42	71.79%	72.69%	75.01%	73.92%	73.28%	71.07%
db43	71.81%	72.76%	74.95%	73.97%	73.24%	71.04%
db44	71.74%	72.74%	75.01%	73.93%	73.30%	71.02%
db45	71.81%	72.75%	75.00%	73.96%	73.31%	70.95%
sym2	72.25%	73.37%	75.65%	74.50%	74.45%	70.76%
sym5	72.22%	73.27%	75.41%	74.21%	74.28%	70.72%
sym10	71.98%	73.38%	75.40%	74.29%	74.10%	70.69%
sym15	72.00%	73.36%	75.21%	73.91%	74.18%	70.69%
sym20	71.98%	73.39%	75.28%	74.03%	74.20%	71.08%
sym25	71.99%	73.51%	75.20%	73.98%	74.24%	71.03%
bior1.1	72.39%	73.43%	75.65%	74.56%	74.37%	70.85%
meyer	71.76%	73.50%	75.35%	74.06%	74.21%	71.10%
bior1.3	72.14%	73.20%	75.39%	74.39%	74.38%	70.53%
bior1.5	71.95%	73.06%	75.22%	74.28%	74.25%	70.40%
bior2.2	70.97%	72.14%	74.38%	73.83%	73.12%	69.46%
bior2.4	70.75%	72.14%	74.26%	73.66%	72.97%	69.37%
bior2.6	70.61%	72.06%	74.13%	73.54%	72.88%	69.25%
bior2.8	70.51%	72.04%	74.05%	73.36%	72.77%	69.21%
bior3.1	69.09%	70.48%	72.38%	72.52%	71.28%	67.54%
bior3.3	69.29%	70.57%	72.57%	72.62%	71.35%	67.85%
bior3.5	69.26%	70.66%	72.61%	72.59%	71.38%	67.86%
bior3.7	69.17%	70.65%	72.58%	72.52%	71.31%	67.81%
bior3.9	69.12%	70.62%	72.47%	72.44%	71.26%	67.81%
bior4.4	71.82%	73.12%	75.39%	74.37%	74.06%	70.57%
bior5.5	**72.94%**	**74.14%**	**76.12%**	**74.79%**	**74.88%**	**71.55%**
bior6.8	71.71%	73.02%	75.22%	74.17%	73.99%	70.41%

V. CONCLUSION

In this paper, SAR image compression system using optimum threshold based SVM with and without wavelets are proposed. It is observed that the images are compressed by 67.81 – 77.36% on using the proposed optimum threshold based system and the performance is evaluated using different wavelets too.

REFERENCES

[1] Drucker, H., Wu, D., Vapnik, V.N.: Support vector machines for spam categorization, IEEE Trans. Neural Networks, 1999, 10, (5), pp. 1048-1054.

[2] Manikandan J and Venkataramani B, "Design of a real time automatic speech recognition system using Modified One Against All SVM classifier," Microprocessors and Microsystems, Volume 35, Issue 6, August 2011, pp. 568-578.

[3] A. Shilton, S. Rajasegarar, C. Leckie and M. Palaniswami, "DP1SVM: A dynamic planar one-class support vector machine for Internet of Things environment," Recent Advances in Internet of Things (RIoT), 2015 International Conference on, Singapore, 2015, pp. 1-6.

[4] I. Nakanishi and Y. Sodani, "SVM-Based Biometric Authentication Using Intra-Body Propagation Signals," Advanced Video and Signal Based Surveillance (AVSS), 2010 Seventh IEEE International Conference on, Boston, MA, 2010, pp. 561-566.

[5] C. He, Y. Li, Y. Huang, C. Liu and S. Fei, "Relevance Vector Machine Based Gear Fault Detection," Pattern Recognition, 2009. CCPR 2009. Chinese Conference on, Nanjing, 2009, pp. 1-5.

[6] A. R. B. Tashk, A. Sayadiyan and S. Valiollahzadeh, "Face Detection Using Adaboosted RVM-based Component Classifier," Image and Signal Processing and Analysis, 2007. ISPA 2007. 5th International Symposium on, Istanbul, 2007, pp. 351-355.

[7] Y. Meiying, "RVM-based nonlinear dynamic compensation of sensors," Control Conference (CCC), 2012 31st Chinese, Hefei, 2012, pp. 3960-3963.

[8] L. B. Tran and T. H. Le, "Personal Authentication Using Relevance Vector Machine (RVM) for Biometric Match Score Fusion," Knowledge and Systems Engineering (KSE), 2015 Seventh International Conference on, Ho Chi Minh City, 2015, pp. 7-12.

[9] A. S. Yommy, R. Liu, S. O. Onuh and A. C. Ikechukwu, "SAR image despeckling and compression using K-nearest neighbour based lee filter and wavelet," 2015 8th International Congress on Image and Signal Processing (CISP), Shenyang, 2015, pp. 158-167.

[10] X. Zhan, R. Zhang, D. Yin and C. Huo, "SAR Image Compression Using Multiscale Dictionary Learning and Sparse Representation," in IEEE Geoscience and Remote Sensing Letters, vol. 10, no. 5, pp. 1090-1094, Sept. 2013.

[11] Jayachandran M and Manikandan J, "SAR Image Compression Using Steganography," Advances in Computer Engineering (ACE), 2010 International Conference on, Bangalore, Karnataka, India, 2010, pp. 203-206.

[12] W. Aili, Z. Ye and G. Yanfeng, "SAR Image Compression Using HVS Model," 2006 CIE International Conference on Radar, Shanghai, 2006, pp. 1-4.

[13] Nishanth VA and Manikandan J, "SAR image compression using Relevance Vector Machines," 2015 Annual IEEE India Conference (INDICON), New Delhi, India, 2015, pp. 1-5.

[14] Stephane Mallat, "A Wavelet Tour of Signal Processing", Academic Press, Third Edition, 2009.

[15] L. Chun-Lin, "A Tutorial of the Wavelet Transform", Department of Electrical Engineering, National Taiwan University, Taipei, Taiwan, 2010.

[16] The USC-SIPI Image Database, University of Southern California, http://sipi.usc.edu/database/

[17] Manikandan J, Venkataramani B and Jayachandran M, "Evaluation of edge detection techniques towards implementation of automatic target recognition", International Conference on Computational Intelligence and Multimedia Applications, 2007, pp. 441-445.